Polym. Korea, Vol. 47, No. 3, pp. 288-302 (2023)
https://doi.org/10.7317/pk.2023.47.3.288

ISSN 0379-153X(Print)
ISSN 2234-8077(Online)

개질된 Nanographene Oxide기반의 실리콘 고무 복합체의 기계적 물성 및 Swelling 거동 연구

V. Aravinth, G. Gurumoorthi, S. Vishvanathperumal*,†, and V. Navaneethakrishnan

Department of Mechanical Engineering, E.G.S. Pillay Engineering College
*Department of Mechanical Engineering, S.A Engineering College

(2022년 11월 19일 접수, 2023년 1월 28일 수정, 2023년 2월 13일 채택)

Effect of Modified Nanographene Oxide on the Mechanical and Swelling Properties of Silicone Rubber Nanocomposites

V. Aravinth, G. Gurumoorthi, S. Vishvanathperumal*,†, and V. Navaneethakrishnan

Department of Mechanical Engineering, E.G.S. Pillay Engineering College, Nagapattinam, Tamilnadu 611002, India
**Department of Mechanical Engineering, S.A Engineering College, Chennai, Tamilnadu 600077, India*

(Received November 19, 2022; Revised January 28, 2023; Accepted February 13, 2023)

Abstract: Nanocomposites were created by using nanographene oxide (GO) as a reinforcing filler into silicone rubber and evaluating the materials' mechanical and abrasion resistance properties. GO was treated with 4,4'-diphenylmethane diisocyanate (MDI), then mixed with phenyl silicone rubber (PSR) at different concentrations (2-10 phr) and vulcanised. It was investigated the impact of MDI modified GO concentration on the morphology of PSR nanocomposites. The swelling properties of silicone rubber/MDI modified GO nanocomposites were also investigated in relation to penetrants (aromatic, aliphatic, and chlorinated solvents) and nanofiller concentrations (0-10 phr). Due to greater dispersion and reinforcing impact, mechanical parameters (tensile strength and modulus), and swelling resistance of silicone nanocomposites improve with MDI-GO concentration. The rate of rise is constant up to a concentration of 6 phr MDI-GO, after which it drops, confirming the formation of agglomeration. The MDI modification of GO improves the dispersion of MDI-GO in silicone rubber considerably, according to FESEM analysis. Because of its strong contact with the polymer matrix, GO serves as reinforcement. This research expands the range of applications for GO in the silicone rubber sector.

Keywords: silicone rubber, nanographite oxide, 4,4'-diphenylmethane diisocyanate, mechanical properties, swelling resistance.

Introduction

Thermoplasts,[1] thermosets,[2] and elastomers[3] are some of the most often used polymer matrices. Elastomers, which include diene rubbers[4] and silicone rubber,[5] are the most investigated polymer family. Because of its high fracture strain, low viscosity, strong dielectric characteristics, and easy processibility, silicone rubber is the most often used rubber.[6] Silicone rubber, with its [-SiRR′-O-] repeat structure, is one of the most imperative non-carbon backbone rubbers. Silicone rubber offers a variety of unique features due to the unique structure of its backbone,[7] including good chemical and ozone resistance, and mechanical stabilities, and outstanding UV over a wide range of humidity and temperature.[8-9] The strength of virgin silicone rubber without filler is often low. The most conventional reinforcing fillers to improve mechanical properties and performance are carbon black and silica.[10-11] However, a significant amount of conventional fillers would hasten the ageing of rubbers because the inner friction of the filler-molecular and filler-filler chain causes high heat build-up potential that cannot be discharged in time. Some researchers proposed employing carbon-based nanofiller as a co-filler to fortify the rubber matrix in order to reduce adverse effects.[12] The most promising choices for flexible devices and components are polymer composites, yet they have inappropriate qualities on their own. As a result, nanofillers are used to improve the polymer matrix's poor characteristics. Carbon allotropes, such as sp^2 hybridised 1D carbon nanotubes (CNTs),[13] 2D graphene,[14] or 3D graphite,[15]

†To whom correspondence should be addressed.
vishvamechanical@gmail.com, ORCID 0000-0001-5935-1444

are often used as nanofillers.

Due to Vander-Waals interactions, nanographene acts as a lubricant and can increase the fracture strain and stretchability in rubber nanocomposites at very low concentrations. Due to their low density, outstanding mechanical properties, high thermal conductivity, and high electron mobility, a low content of nanofillers produces a significant enhancement in electrical and mechanical properties.[16] Carbon nanomaterials (CNTs, graphene, and graphite) have been used in a variety of applications, including transparent conductors, nanoelectronic devices, drug delivery, biomolecular detection, and so on.

To improve the electrical and thermal properties of elastomeric matrices, nanographene oxide (GO) is utilised as a precursor. Although these nano sheets exhibit high mechanical properties in elastomeric matrices, they can be used as a matrix stiffening agent.[17-18] The surface of graphene nano sheets is functionalized with appropriate agents to increase dispersion in different solvents (aromatic, aliphatic and chlorinated) and compatibility with elastomer matrices. These materials can be disseminated in polar solvents due to the presence of epoxies, hydroxyl groups on the surface of nano sheets and carbonyl, carboxyl groups at the edges of GO sheets.[19-20] Many research have been conducted on the dispersion of GO in nonpolar media. Tang *et al*.[21] used alkylated melamine (ADDT) produced from cyanuric chloride to covalently functionalize the surface of GO nano sheets. The GO-ADDT that resulted was quite soluble in organic solvents. He investigated the thermal stability of GO-ADDT and discovered that it had a higher thermal resistance than GO. For dispersion of GO in n-octane solvent, Yu *et al*.[22] employed a phase transfer approach. He used oleylamine as a suspending agent in the solvent for this. As a result, oleylamine and GO developed a robust connection. FTIR spectra confirmed the presence of oleylamine on the GO sheets. Decyl groups were added to a variety of imperfection sites on the surface of reduced GO by Tessonnier *et al*.[23] and Huang *et al*.[24] As a result, polar GO disseminated in non-polar solvents like toluene. He discovered that the presence of these alkyl chains can inhibit graphene sheets from re- agglomeration in non-polar media.

Kim *et al*.[25] methods of treating GO with phenyl isocyanate and subsequently incorporating this modified GO with polyurethane increased the electrical conductivity and gas barrier of the nanocomposites. GO was used by Deshmukh *et al*.[26] to improve the thermal and mechanical characteristics of polyvinylchloride (PVC). To improve the thermal stability of the nano-composites, Wang *et al*.[27] produced GO/silicone rubber nano-composites. Functionalized graphene sheets (FGSs) are used by Ozbas *et al*.[28] to increase the mechanical characteristics, electrical conductivity, and gas permeability of polydimethylsiloxane (PDMS). The conductivity of composites revealed electrical percolation at 0.8 wt% FGS. Gan *et al*.[29] used graphene nanoribbon to improve the mechanical and thermal properties of silicone rubber nanocomposites. To our knowledge, no studies on the effect of GO on the mechanical properties and swelling resistance of phenyl silicone rubber (PSR) have been published. GO is a two-dimensional carbon sheet that was created using a modified Hummers process from natural graphite oxide. The GO can disperse in water and form a stable colloid solution due to the abundance of oxygen-containing groups on its surface. This allows for the creation of a new category of solution-dispersible aromatic hydrocarbons platforms for chemical reactions. On either side of the basal plane, GO has covalent link epoxide and hydroxyl functional groups, whereas carboxyl groups are found at the edge sites.[30] The surface property of GO may shift from non-polar to polar due to the presence of oxygen-containing functional groups, enhancing the adsorption of ionic and non-ionic contaminants.[31] Organic pollutants could be absorbed by GO *via* hydrogen bonds, electron donor–acceptor interactions, and dispersive interactions.[32-33]

The aim of this analysis was to investigate 4,4′-diphenylmethane diisocyanate (MDI) modified GO as reinforcement for the silicone rubber. To achieve homogeneous dispersion of MDI-GO in the PSR matrix, GO was first produced using a modified Hummers process and then treated with MDI. After that, MDI-GO was mixed with PSR in an open two-roll mill mixer using dicumyl peroxide as a vulcanizing agent. The differences in curing, mechanical, abrasion, swelling, and morphology properties were examined and compared to pure silicone rubber.

Experimental

Materials. All of the other chemicals (sodium nitrate ($NaNO_3$), sulphuric acid (H_2SO_4), potassium perman-ganate ($KMnO_4$), hydrogen peroxide (H_2O_2), hydrochloric acid (HCl), dibutyltin dilaurate ($C_{32}H_{64}O_4Sn$), acetone, and solvents (benzene - C_6H_6, xylene - C_8H_{10}, toluene - C_7H_8, dichloromethane - CH_2Cl_2, mesitylene - C_9H_{12}, n-hexane - C_6C_{14}, n-pentane - C_5H_{12}, n-octane - C_8H_{18}, n-heptane - C_7H_{16}, carbon tetrachloride - CCl_4, and chloroform - $CHCl_3$) were of exploratory grade and were used without further decontamination and were purchased from Sigma-Aldrich, Puducherry, India.

Preparation of Graphene Oxide. First, a modified Hum-

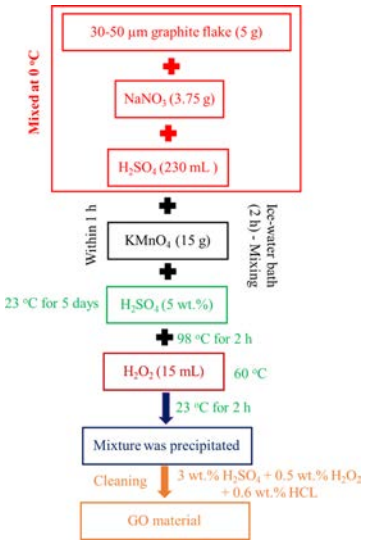

Figure 1. Preparation of graphene oxide.

mers technique was used to create graphene oxide (GO).[34] Figure 1 shows the preparation of graphene oxide. At 0 ℃, 5 g of 30-50 µm graphite flake, 3.75 g $NaNO_3$, and 230 mL H_2SO_4 were united. Within 1 h, 15 g $KMnO_4$ was progressively added to the mixture, followed by two hours of stirring in an ice-water bath. Half liter of 5 wt% H_2SO_4 was added in one hour after additional stirring at 23 ℃ for five days. At 98 ℃, the resulting mixture was agitated for another 2 h. The temperature was then reduced to 60 ℃, and 15 mL of dilute hydrogen peroxide (H_2O_2) were added. After being agitated for two hours at 23 ℃, the mixture was precipitated, then cleaned several times with an aqueous solution of 3 wt% H_2SO_4/0.5 wt% H_2O_2 and filtered. The resulting solid was then rinsed three times with a 3 wt% and 0.6 wt% HCl solution. The GO material was then filtered and dried for a week in a vacuum oven after being rinsed with deionized water until the pH was nearly 7.[35,36]

Preparation of Modified GO. Figure 2 shows the preparation of modified graphene oxide. GO was dried or dehydrated for 3 h at 80 ℃ in a vacuum oven. GO was ultrasonically sonicated in anhydrous *N*,*N*-dimethylacetamide (DMAc) to produce a homogeneous dispersion. The mixture was heated to 80 ℃ while being agitated under nitrogen. After MDI was dissolved in anhydrous DMAc, a few drops of dibutyltin dilaurate (DBTDL) were added to the dispersion. For 4 h, the reaction was held at 80 ℃. The mixture was centrifuged and repeatedly washed with acetone to remove any remaining MDI after cooling to room temperature. A vacuum oven at 50 ℃ was used to dry the solid product for 24 h. The process of GO functionalization by MDI is depicted in Figure 3.

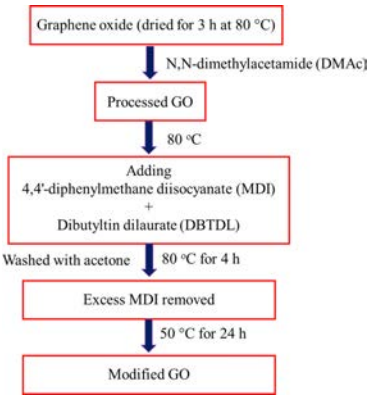

Figure 2. Preparation of MDI-GO.

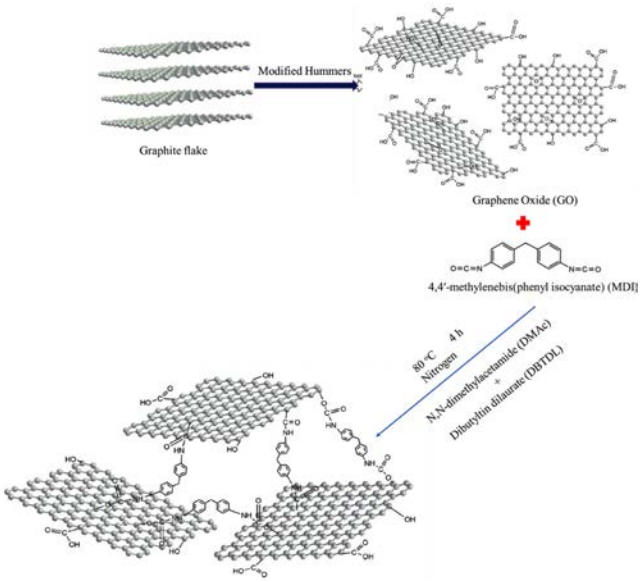

Figure 3. Schematic representation of the MDI-GO synthesis process.[37]

Preparation of Silicone/GO Nanocomposite. To prepare the required sample, a silicone elastomer was utilised, which was mixed with other substances in a laboratory-sized open mill mixing equipment with a speed ratio of 1:1.4, according to ASTM D-3182 guidelines. (i) Silicone rubber - 100 phr; (ii) MDI modified GO - varied (0, 2, 4, 6, 8, and 10 phr); (iii) dicumyl peroxide - 4 phr are utilised in the mixing of components and their proportions. The temperature was kept between 60 and 70 ℃ throughout the mixing process, as were the mixing time (15-25 min), nip gap (1-2 mm), and cutting processes (for proper mixing of rubber, reinforcement and vulcanizing agent). The prepared samples were then electrically heated and moulded in a semi-automated hydraulic press under the same conditions (pressure: 30 MPa, temperature: 160 ℃, and time: optimal cure time).[38] Figure 4 shows the schematic diagram of sample

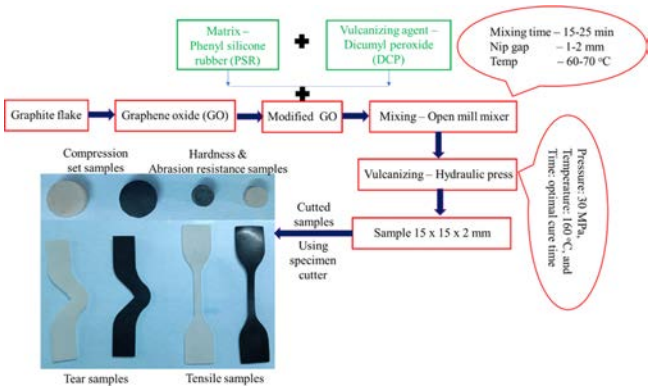

Figure 4. Preparation of silicone rubber/GO nanocomposite.

preparation.

Characterizations. The nanocomposites' cure rate index (CRI): CRI (min^{-1}) = 100/(t_{s2}-t_{90}), scorch time (t_{s2}, min), cure time at 90% (optimum cure time, t_{90}, min), minimum torque (M_l, dNm), maximum torque (M_h, dNm), and torque difference (ΔM, dNm) were all measured from an ODR (oscillating die rheometer) equipment with ASTM D-2048 at a temperature of 160 ℃.

The tensile characteristics were assessed using Instron 4302 testing equipment at room temperature (23 ℃) in accordance with ASTM D-412.[39] Using the same machine, the tear strength of the rubber nanocomposites was tested according to ASTM D-624 standard testing.[40] All specimens were tested at 500 mm/min for tensile and tear strength. To reduce the random mistake, the tear and tensile operation was done five times. Shore A durometer were used to determine hardness in accordance with ASTM D-2240. The rebound resilience of all rubber nanocomposites was tested using ASTM D-2632 methods by vertical rebound resilience of each sample. The nanocomposites' abrasion resistance was measured with a DIN abrader and grade 60 emery paper at ambient (23 ℃) temperature, 10 N force (constant), and 0.32 m/s speed (constant). The ASTM D-5963 standard was used to investigation of abrasion resistance in terms of volume loss. The compression set sample was made into a button shape with a ϕ29 mm and a 12 ± 0.5 mm thickness. A compression device was used to measure the permanent compression set. The specimens were pressed for 1 day, 2 days, and 3 days at 23 ℃ with a 25% deformation rate. The specimen was then taken out of the compression device and given 30 minutes to rest at room temperature. It was determined that the permanent compression set (C) was

$$\text{Permanent compression set (C)} = \frac{H_0 - H_1}{H_0 - H_n} \times 100\% \quad (1)$$

where, H_0 - original height, H_1 - final height of the sample and H_n - spacer height.

The solvent immersion method was used to perform the swelling test as per standard ASTM D-471. The samples were sliced in the shape of squares with round edges (with a size of 25 mm and a 2 mm thickness) from a sheet of rubber nanocomposites to analyse the behaviour of silicone/MDI-GO nanocomposites after swelling. Following that, the weight of each sample was determined using highly sensitive weighing equipment, and the samples were placed in different solvents for various periods of time. Dichloromethane, benzene, xylene, toluene, mesitylene, n-hexane, n-pentane, n-octane, n-heptane, carbon tetrachloride, and chloroform were the solvents employed in this experiment. The samples were taken out of the solvent, cleaned, and weighed again once the time limit had expired. The following equation was used to compute the mole percent uptake:

$$Q_t = \frac{(M_t - M_0)/MW}{M_0} \times 100 \quad (2)$$

where, MW - molecular weight of the penetrant, M_0 - samples weight before swelling, and M_t - swelled samples weight after time 72 h of immersion.

Micro-photomicrographs taken with a SEM were used to investigate the morphological aspects of silicone nanocomposites (ZEISS EVO 18 MA s SEM). Before that, the samples were sputter-coated with gold.

The thermal ageing characteristics of silicone nanocomposites were investigated by ageing for 96 h at 70 ℃ (the rest for a similar time at 100 ℃ and 125 ℃, as per ASTM D-865) and 100 ℃ and 125 ℃ as per ASTM D-573. After a 96 h ageing test, the parameters of accelerated ageing were measured. After ageing, the silicone nanocomposites' tensile strength, 100% modulus, tear strength, elongation at break, abrasion resistance, hardness and rebound resilience were assessed to estimate ageing resistance. The percentage of retention in specimen properties is determined as follows:

$$\text{Percentage retention} = \frac{\text{Value after aging}}{\text{Value before aging}} \times 100 \quad (3)$$

Results and Discussion

Cure Properties of Silicone Nanocomposites. The cure properties of the rubber compounds are very important parameter where the material for utilization is to be molded. Cure characteristics such as M_l, M_h, ΔM, t_{s2}, t_{90}, and CRI can be used

Table 1. Cure Properties of the Silicone Rubber Reinforced with MDI Modified GO Composites

Sample code	Min. torque (M_l) (dN m)	Max. torque (M_h) (dN m)	Torque difference (ΔM) (dN m)	Scorch time (t_{s2}) (min)	Optimum cure time (t_{90}) (min)	Cure rate index (CRI) (min^{-1})
MDI-GO_0	4.21	48.15	43.94	2.56	15.26	7.87
MDI-GO_2	4.35	49.64	45.29	2.35	14.86	7.99
MDI-GO_4	4.48	51.95	47.47	2.13	14.32	8.2
MDI-GO_6	4.96	54.78	49.82	1.98	12.26	9.73
MDI-GO_8	5.11	55.82	50.71	1.95	12.5	9.48
MDI-GO_{10}	4.72	55.48	50.76	2.5	12.3	10.2

to estimate the processability of nanocomposites. For silicone rubber nanocomposites containing different concentrations of MDI modified GO (MDI-GO), the cure time for curing compounds was evaluated, as well as the differences in cure time for different loadings.

Table 1 presents the outcomes for curing times and torque values of the silicone rubber nanocomposites. Except for 10 phr MDI-GO content, which exhibited a scorch time equivalent to pure silicone rubber, the t_{s2} of silicone rubber nanocomposites reduced with increasing MDI-GO content. The reduction in t_{s2} durations might be attributed to the silicone compound's higher frictional heat during the ODR testing process, which sped up the curing process by increasing the amount of MDI-GO in the silicone compound. The optimum cure time (vulcanizing periods) of the silicone rubber nanocomposites, on the other hand, behaved differently, initially decreasing when MDI-GO content was incorporated into the mixtures and then increasing as the MDI-GO level increased from 8 to 10 phr. This behaviour was seen because an acceptable proportion of MDI-GO content in the silicone rubber nanocomposites might operate as a co-curing material during the chemical vulcanizing process, resulting in a reduction in cure periods at first. However, as the concentrations of MDI-GO increased, they hinder the principal vulcanizing agent's activity, resulting in longer cure durations. It's worth noting that the silicone nanocomposites containing 10 phr MDI-GO had particularly stumpy scorch and cure times. This could be because MDI-GO has a higher filler-filler interaction and agglomeration than 4 phr and 6 phr, resulting in a higher content with the MDI-GO nanofiller, obstructing the vulcanizing agent's operations. The cure rate index (CRI) (rate of curing activity) showed an increased trend, as shown in Table 1. This improvement is more obvious in MDI-GO nanofillers filled silicone rubber nanocomposites, which could be attributed to a significant improvement in the interfacial rubber-nanofiller contact, which leads to improved rheometric characteristics.

The viscosity of the compounds is interconnected to the M_l (*i.e.* the torque at the commencement of vulcanization). Table 1 shows the M_l of nanocomposites loaded with various concentrations of MDI-GO. With MDI-GO loadings up to 8 phr, the minimum torque increased. Because torque is related to stiffness, the results showed that increasing the amount of MDI-GO in the rubber matrix enhances the vulcanizate's stiffness.[41-43] The highest torque indicates the fully vulcanised rubber's shear modulus at the vulcanization temperature, which increases with filler loading. The maximum torque definitely increases with increased MDI-GO loading in the nanocomposite, although the maximum torque increased up to 8 phr before dropping in silicone nanocomposites loaded with higher amounts of MDI-GO. This rise was an indirect indicator of better silicone/MDI-GO interfacial adhesion. These findings confirmed that the addition of treated graphene oxide (MDI-GO) in silicone rubber affects the processability of the nanocomposite and thus the treated GO can act as a reinforcement agent for the matrix after a further increase in MDI-GO loading (*i.e.* 10 phr) and agglomeration of the nanofiller in the silicone rubber matrix.

With increasing MDI-GO content, the ΔM increased in Table 1, which could circuitously reflect to the crosslink density of the silicone nanocomposites. This rise in torque difference could be explained by the fact that these MDI-GO served as a co-vulcanizing agent during the chemical vulcanization progression. Additional elucidation for the increased ΔM could be that MDI-GO molecules are substantially stiffer than silicone rubber molecules, resulting in higher nanocomposites viscosity when more MDI-GO was added during the compounding process.

Mechanical Properties of Silicone Nanocomposites. As shown in Figure 5, increasing MDI-GO concentration increased the 100% tensile modulus and hardness (Shore A), with stronger impacts on 10 phr GO/silicone rubber nanocomposites. The high stiffness of the MDI-GO nanofiller used in this study

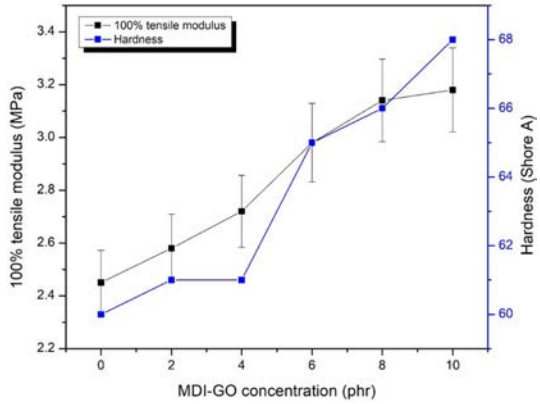

Figure 5. 100% tensile modulus and hardness of silicone rubber with MDI-GO composites.

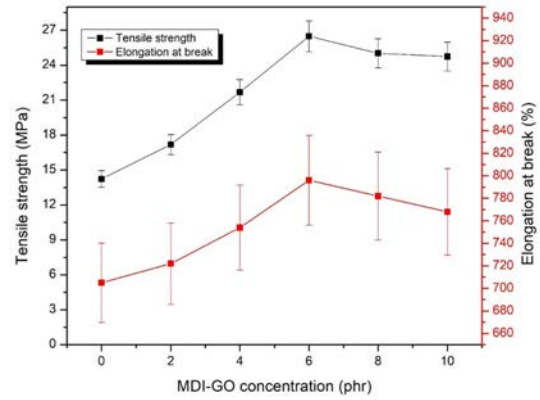

Figure 6. Elongation at break and tensile strength of PSR with MDI-GO composites.

may have increased the torque difference and crosslink density of the silicone nanocomposites, limited the crosslink joints of the inter-crosslink chains and raised the overall rigidity of the silicone rubber nanocomposites.

However, as seen in Figure 6, the PSR nanocomposites behaved differently in terms of elongation at break and tensile strength. When 6 phr MDI-GO was added to the silicone rubber nanocomposites, their values continuously increased; however, when more MDI-GO content was added, the values diminished. These results were seen because the MDI-GO might act as a co-vulcanizing agent with sufficient MDI-GO addition, resulting in a higher crosslink density and elongation at break/tensile strength. However, as more MDI-GO was incorporated to the PSR nanocomposites, more favourable rubber-filler interactions were replaced, resulting in agglomeration of MDI-GO nanofillers and poor particle dispersion.

The tear strength of PSR-modified GO nanocomposites is exposed in Figure 7. The tear strength of pristine silicone rubber is 32.15 N/mm, and the tear strength increases steadily as the modified GO concentration in the polymer matrix increases. Maximum increase in tear strength is achieved at 10 phr modified GO concentration of 44.87 N/mm. The increased tear strength of nanocomposites shows that when modified GO is placed in the rubber polymer matrix, the resistance to tear is increased.

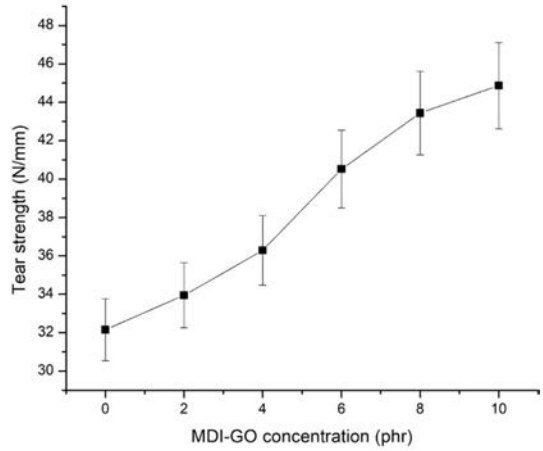

Figure 7. Tear strength of PSR with MDI-GO composites.

The ratio of the indenter's energy after impact to its energy before impact, stated as a percentage, is called rebound resilience. In general, the rebound resilience values examined in the vertical rebound resilience tester experiment had approval significant effect on MDI modified GO, as shown in Figure 8. The rebound resilience of silicone nanocomposites with MDI-GO included from 0 to 10 phr was reduced by roughly 31%. This could be because the value of hardness has increased, resulting in a lower value for rebound resilience.[44] Hardness

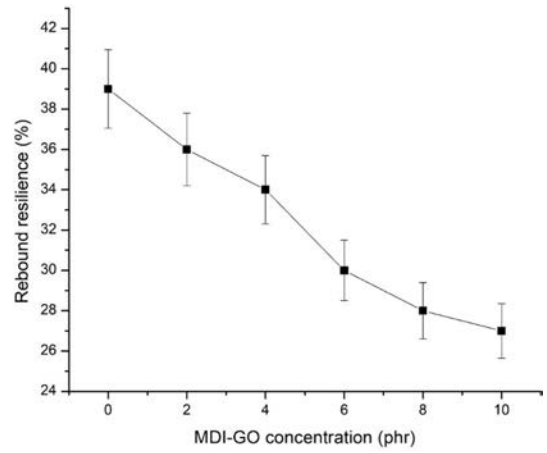

Figure 8. Rebound resilience of silicone rubber with MDI-GO composites.

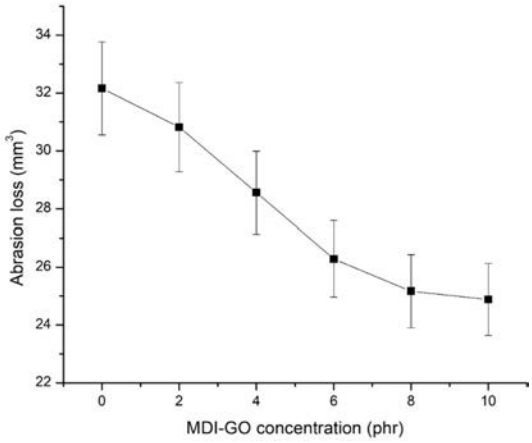

Figure 9. Abrasion loss of silicone rubber with MDI-GO composites.

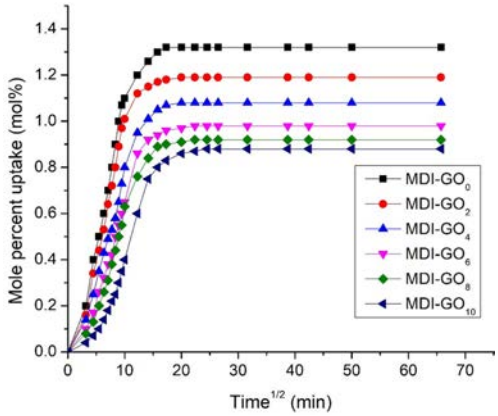

Figure 10. Mole percent uptake of toluene by different MDI-GO content at 23 ℃.

and rebound resilience have an adverse connection, according to Ganeche *et al.*[45]

Figure 9 shows the findings from an investigation into the abrasion resistance of MDI modified GO filled silicone nanocomposites, expressed as an abrasion loss. Silicone nanocomposites' abrasion resistance improves as the MDI modified GO content rises. Reduced abrasion loss in silicone nanocomposites indicates that modified GO functions as a reinforcing filler that interacts better with the rubber matrix. This improvement may be attributable to greater surface area and improved rubber-filler interfacial adhesion, both of which help to increase abrasion resistance.

Swelling Study. Over the course of their lives, polymers are subjected to a variety of chemical environments and are used in a variety of applications, including barrier applications. The swelling curves are presented as a function of the polymer's mole percent uptake (Q_t) *vs*. the √time ($t^{1/2}$). On mole percent uptake through silicone nanocomposites, the impacts of MDI modified GO loading and type of penetrants were investigated. Generally, the swelling behaviour of rubber compounds is influenced by the types and nature of fillers, kinds of matrix, solvent-matrix reaction, temperature, and other factors.

Figure 10 depicts the mole percent toluene uptake by various MDI-GO loadings crosslinked with dicumyl peroxide at 23 ℃. When MDI-GO filled nanocomposites are compared to unfilled compounds, toluene absorption is reduced. The graph clearly demonstrates that silicone rubber has the maximum equilibrium absorption, and that as MDI-GO is included into nanocomposites, the mole percent uptake drops. The swelling of the penetrant solvent depends on the amount of open space in the elastomeric matrix material available to accept the penetrant molecule. Due to the addition of MDI-GO, these permitted spaces in the silicone rubber matrix were less accessible, which restricted segmental mobility and made it difficult for penetrant molecules to penetrate through the nanocomposites. Table 2 shows that aromatic, aliphatic, and chlorinated solvents all follow the same pattern.

The mole percent uptake of all aliphatic solvents via 10 phr MDI modified GO filler filled silicone rubber nano-composites is shown in Figure 11 as a function of penetrant size. According to the graph, the pattern is as follows: n-octane < n-heptane < n-hexane < n-pentane. The penetrant molecule with the bottommost molecular weight (MW) has the maximum uptake, while the solvent with the largest MW has the lowest absorption. The MW and solvent penetrant are usually inversely proportional. Table 2 shows that aromatic and chlorinated solvents follow the similar pattern.

Compression Set Properties. To determine the impact of MDI-GO loading on the compression set behaviour of silicone

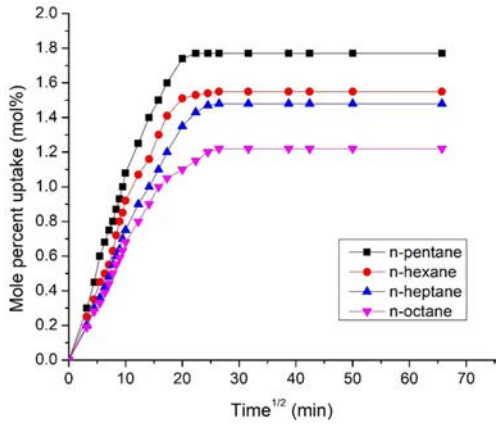

Figure 11. Mole percent uptake of various solvents via silicone rubber nanocomposites loaded with 10 phr MDI-GO.

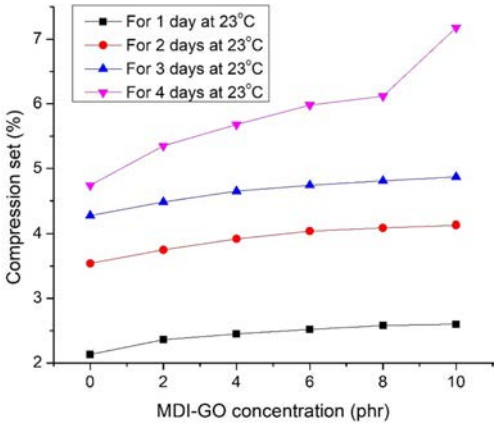

Figure 12. Compression set of silicone rubber with MDI-GO composites.

nanocomposites, the compression set experiment was carried out under various circumstances (at 23 ℃ for 1, 2, 3, and 4 days). The capacity of the rubber to maintain its elastic properties after prolonged compression at a severe strain under the specified conditions is measured by the compression set, a permanent set of elastomeric compounds.[46-47] Figure 12 shows the different compression circumstances for silicone nanocomposites loaded with modified GO loading on the compression set. The compound's compression set rises with increased MDI-GO loading. In unfilled rubber compounds, the compression set is insignificant; nevertheless, when the MDI-GO loading rises, the compression set also does. This occurs as a result of the crosslinking density rising together with the MDI-GO loading. Therefore, make the MDI-GO loaded compounds stiffer. Crosslink density increases as a result, producing a high compression set. At 23 ℃, a similar pattern emerged in the compression set test (for 2, 3, and 4 days). The compression set increases as the number of day's increases. The duration of the holding period (days) has a significant impact on the permanent set and significantly affects the sustainable qualities. The ability to maintain elastic properties improves with decreasing compression set. The better the material for usage, the lower the compression set.

Thermal Ageing Study. At room temperature (from approx. 15 to 40 ℃ in India country), the action of atmospheric oxygen or other gases on silicone rubber compounds is very low impact, nonetheless Heat can perform this action. Thermal aging of compounds is the worsening of advantageous characteristics during service or storage environments; i.e., common phenomenon to a wide variety of natural rubber and synthetic rubber (SBR, EPDM, NBR, etc.), including silicone rubber.[48] Rubber components can undergo a variety of changes as a result of the conditions in which they are used or kept.[49-50] Determine the aged values of the cured rubber's mechanical properties by ageing the materials at 70, 100, and 125 ℃ for 72 h (3 days) to 144 h (6 days). The mechanical characteristics of cured rubber samples were examined after they were aged at high (70 ℃, 100 ℃ and 125 ℃) temperatures for 96 h. Changes in physical qualities such as modulus of elasticity, tensile strength and hardness are industrially relevant features of ageing. If the conditions are too extreme, the rubber may become unusable quickly.

Like all polymeric materials, silicone rubbers are susceptible to deterioration over time when subjected to a variety of environmental and chemical attackers (as described in section 3.3) and extreme temperatures.[51-52] Aging causes a material's desired qualities to deteriorate, eventually leading to failure,[53] which can be disastrous or result in severe financial loss. Understanding the impact of ageing on material properties is therefore critical for predicting product lifetimes and continuously improving products and processes.[54] Accelerated thermal ageing examinations are commonly used to determine the extent of material property changes. Researchers in academia and industry have been interested in such studies in order to gather quantitative

Table 2. Mole Percent Uptake of Penetrant (aromatic, aliphatic and chlorinated) *via* Silicone Rubber Reinforced with MDI-GO Composites at 23 ℃

Sample code (Sam)	Mole percent uptake (mol%) at 23 ℃										
	Aromatic				Aliphatic				Chlorinated		
	C_6H_6	C_7H_8	C_8H_{10}	C_9H_{12}	C_5H_{12}	C_6C_{14}	C_7H_{16}	C_8H_{18}	CH_2Cl_2	$CHCl_3$	CCl_4
MDI-GO_0	1.63	1.32	1.17	1.08	2.13	1.86	1.75	1.48	1.46	2.56	1.58
MDI-GO_2	1.51	1.19	1.03	0.93	2.02	1.75	1.68	1.41	1.38	2.28	1.45
MDI-GO_4	1.38	1.08	0.94	0.85	1.95	1.68	1.61	1.34	1.31	2.15	1.34
MDI-GO_6	1.27	0.98	0.85	0.74	1.86	1.62	1.55	1.28	1.25	2.08	1.28
MDI-GO_8	1.25	0.92	0.77	0.71	1.82	1.58	1.51	1.25	1.17	2.04	1.24
MDI-GO_{10}	1.22	0.88	0.74	0.68	1.77	1.55	1.48	1.22	1.15	1.98	1.18

and qualitative data on the enduring arrangement of materials in various service settings. The three main objectives of accelerated ageing are to (i) choose the optimal material for the specific environment and exposure period, (ii) identify degradation mechanisms in service prior to the application, and (iii) predict a material's service life and activity over time.[55] However, as more and more SRs are used in various industrial machinery and process applications, it is crucial to comprehend the changes in characteristics brought on by in-service conditions over time. These studies can be used by engineers to avoid unforeseen machine breakdowns and process interruptions. For instance, recent research has looked into the ageing of SR in respect to its function as a sealing substance in machinery.[56] At high temperatures, SR components in numerous engineering machines come into touch with lubricants and oils, as well as heat transfer fluids. These factors can have a negative impact on the rubber's characteristics and limit its lifespan.

Although the ageing procedure of SR is complicated, it is well understood that oxidation process is a major degrading mechanism. At higher temperatures, the rate of deterioration is greatly enhanced. The mechanical characteristics of silicone nanocomposites as well as their thermally aged equivalents were measured and compared. At high temperatures, the physical qualities of the silicone rubber compound's final cured products, particularly their mechanical properties, can change. Particularly whether they are used as structural materials or in industrial processes, rubbers' mechanical characteristics are essential to their performance in a number of applications.[57] Rubber samples are often only cured to 90% of their M_h in the industrial setting.[58] To allow for the introduction of crosslinks into the rubber matrix during service, the 10% limit is typically maintained. As a result, the influence of temperature on ageing property must be assessed. Elongation at break (E_b), tensile (T_s) and tear (T_a) strength, hardness (H_d), 100 percent modulus (M_{100}), and rebound resilience (R_r) as well as abrasion resistance (A_r) are also shown in Tables 3, 4, 5, 6, 7, 8, and 9. The obtained thermal aging consequences at three different temperatures, 70, 100, and 125 ℃, for 96 h (4 days) show the onset of sharp values of T_s; M_{100}, T_a, E_b, H_d, R_r, and A_r of silicone nanocomposites filled with different content of MDI-GO at 125 ℃, while those of nanocomposites at 100 ℃ and 70 ℃, a high decrease in T_s, M_{100}, T_a, E_b, H_d, R_r and A_r was noted. On the other hand, at 70 ℃ of aging temperature, the values of T_s, M_{100}, T_s, H_d and A_r increased, while the values of E_b and R_r decreased.

The rate of the aforementioned qualities reduces as the ageing temperature rises from 100 ℃ to 125 ℃; nevertheless, the rate of T_s, M_{100}, and H_d rises as the ageing temperature rises from

Table 3. Effect of MDI-GO Loading on T_s of SR Nanocomposites Before/after Aging

MDI-GO loading	T_s (MPa)						
	Actual value	Aging temperature at 70 ℃ for 4 days (96 h)	Percentage retention	Aging temperature at 100 ℃ for 4 days	Percentage retention	Aging temperature at 125 ℃ for 4 days	Percentage retention
0	14.23	14.75	103.7	15.87	111.5	10.23	71.9
2	17.18	18.84	109.7	20.15	117.3	12.17	70.8
4	21.68	22.96	105.9	24.47	112.9	13.69	63.1
6	26.48	28.54	107.8	30.18	114	14.28	53.9
8	25.02	26.64	106.5	27.54	110.1	12.51	50
10	24.74	25.65	103.7	26.67	107.8	12.08	48.8

Table 4. Effect of MDI-GO Loading on E_b of SR Nanocomposites Before/after Aging

MDI-GO loading	E_b (%)						
	Actual value	Aging temperature at 70 ℃ for 4 days (96 h)	Percentage retention	Aging temperature at 100 ℃ for 4 days	Percentage retention	Aging temperature at 125 ℃ for 4 days	Percentage retention
0	705	598	84.8	530	75.2	408	57.9
2	722	612	84.8	548	75.9	423	58.6
4	754	636	84.4	558	74	432	57.3
6	796	641	80.5	567	71.2	438	55
8	782	615	78.6	523	66.9	398	50.9
10	768	603	78.5	506	65.9	374	48.7

Table 5. Effect of MDI-GO Content on H_d of SR Nanocomposites Before/after Aging

MDI-GO loading	H_d (Shore A)						
	Actual value	Aging temperature at 70 ℃ for 4 days (96 h)	Percentage retention	Aging temperature at 100 ℃ for 4 days	Percentage retention	Aging temperature at 125 ℃ for 4 days	Percentage retention
0	60	61	101.7	63	105	58	96.7
2	61	62	101.6	65	106.6	59	96.7
4	61	63	103.3	68	111.5	60	98.4
6	65	66	101.5	70	107.7	62	95.4
8	66	67	101.5	71	107.6	62	93.9
10	68	70	102.9	73	107.4	63	92.6

Table 6. Effect of MDI-GO Loading on 100% Modulus of Silicone Rubber Nanocomposites Before/after Aging

MDI-GO loading	100% Modulus (MPa)						
	Actual value	Aging temperature at 70 ℃ for 4 days (96 h)	Percentage retention	Aging temperature at 100 ℃ for 4 days	Percentage retention	Aging temperature at 125 ℃ for 4 days	Percentage retention
0	2.45	2.76	112.7	2.94	120	1.96	80
2	2.58	2.84	110.1	3.06	118.6	2.13	82.6
4	2.72	3.03	111.4	3.21	118	2.36	86.8
6	2.98	3.18	106.7	3.35	112.4	2.54	85.2
8	3.14	3.28	104.5	3.4	108.3	2.61	83.1
10	3.18	3.32	104.4	3.48	109.4	2.63	82.7

Table 7. Effect of MDI-GO Loading on T_a of SR Nanocomposites Before/after Aging

MDI-GO loading	T_a (N/mm)						
	Actual value	Aging temperature at 70 ℃ for 4 days (96 h)	Percentage retention	Aging temperature at 100 ℃ for 4 days	Percentage retention	Aging temperature at 125 ℃ for 4 days	Percentage retention
0	32.15	34.26	106.6	34.87	108.5	28.64	89.1
2	33.95	35.17	103.6	36.08	106.3	29.07	85.6
4	36.28	37.88	104.4	38.47	106	29.72	81.9
6	40.52	43.14	106.5	44.12	108.9	30.65	75.6
8	43.44	44.51	102.5	44.98	103.5	30.96	71.3
10	44.87	45.76	102	46.38	103.4	31.05	69.2

Table 8. Effect of MDI-GO Loading on Rebound Resilience of Silicone Rubber Nanocomposites Before/after Aging

MDI-GO loading	Rebound resilience (%)						
	Actual value	Aging temperature at 70 ℃ for 4 days (96 h)	Percentage retention	Aging temperature at 100 ℃ for 4 days	Percentage retention	Aging temperature at 125 ℃ for 4 days	Percentage retention
0	39	35	89.7	33	84.6	30	76.9
2	36	33	91.7	31	86.1	28	77.8
4	34	30	88.2	28	82.4	25	73.5
6	30	25	83.3	24	80	23	76.7
8	28	23	82.1	22	78.6	20	71.4
10	27	22	81.5	20	74.1	17	63

Table 9. Effect of MDI-GO Loading on Abrasion Loss of Silicone Rubber Nanocomposites Before/after Aging

MDI-GO loading	Abrasion loss (mm^3)						
	Actual value	Aging temperature at 70 ℃ for 4 days (96 h)	Percentage retention	Aging temperature at 100 ℃ for 4 days	Percentage retention	Aging temperature at 125 ℃ for 4 days	Percentage retention
0	32.16	31.54	98.1	31.02	96.5	50.25	156.3
2	30.82	28.14	91.3	27.88	90.5	48.14	156.2
4	28.56	27.12	95	26.81	93.9	46.64	163.3
6	26.28	24.65	93.8	24.15	91.9	43.25	164.6
8	25.17	23.98	95.3	23.16	92	42.82	170.1
10	24.88	23.42	94.1	22.98	92.4	42.46	170.7

70 ℃ to 100 ℃. Because of the intricacy of processes taking place in the vulcanized elastomer material, ageing temperature has an effect on T_s, M_{100}, and H_d. Due to decreased molecular weight and molecular entanglement in MDI-GO-filled silicone nanocomposites with high cross-link density, this change in behaviour can also be brought on by polymer chain scission. Through molecular mobility restriction, the latter reduces energy loss. The cross-link density affects the tensile and tear strength qualities of the material. Table 9 shows that the crosslink density of silicone nanocomposites filled with various amounts of MDI-GO nanofillers increases steadily as the MDI-GO content increases. This is a post-vulcanizing impact that tends to get worse as the ageing temperature rises. Clarke *et al.*[59] indicate that both scission and cross-linking reactions increase with increasing ageing temperature in their investigation on ageing kinetics of T_s of natural rubber compound. T_s, T_a, E_b, M_{100}, H_d, R_r, and A_r all decrease with age in samples having varying loadings of MDI-GO-filled and unfilled silicone rubber nanocomposites. After 96 h of ageing at 125 ℃, these characteristics rapidly deteriorate. The decrease in property values indicates deterioration due to accelerated ageing. The characteristics of nanocomposite materials appear to improve as MDI-GO loading increases. Only the rubber portion of a rubber material degrades when it is subjected to high temperatures.[60] When the proportion of MDI-GO in silicone rubber nanocomposites is increased, the degradable rubber component is diluted, resulting in a greater value after age. Accelerated ageing of silicone rubbers with Si-O linkages usually leads in a decrease in their strength qualities.

Tables 3 and 4 show the reduction percentage in T_s and E_b of silicone rubber nanocomposites, and their decreasing (reduction) rate. T_s and E_b of SR nanocomposites fell from 26.48 to 14.28 MPa and from 796 to 438% correspondingly after 4 days (92 h) of exposure to silicone rubber nanocomposites at elevated temperature (125 ℃), equivalent to 53.9 and 55 percent reductions. It's worth noting that at 70 ℃ of ageing, the decline rate of tensile strength shows a considerable stepwise increment of 107.8%, before remaining reasonably steady up to 100 ℃. However, the rate of tensile strength decreased dramatically from 100 ℃ to 125 ℃, reaching only 53.9%. However, at 70 ℃, the reduction rate of elongation at break steadily decreased to 80.5%, then declining sequentially to 71.2% towards the conclusion of 100 ℃. The decrease rate changed significantly from 100 ℃ to 125 ℃. The decline rate of ultimate elongation at break dropped dramatically from 100 ℃ to 125 ℃, similar to tensile strength. These findings suggest that after a specific degree of ageing temperature (100 ℃), the tensile characteristics and elongation at break of silicone rubber nanocomposite are affected by

Table 10. Effect of MDI-GO Loading on υ of SR Nanocomposites Before/after Aging

MDI-GO loading	Crosslinking density (x10^{-3} mol/cc)						
	Actual value	Aging temperature at 70 ℃ for 4 days (96 h)	Percentage retention	Aging temperature at 100 ℃ for 4 days	Percentage retention	Aging temperature at 125 ℃ for 4 days	Percentage retention
0	0.56858	0.640523	112.7	0.682296	120	0.454864	80
2	0.59875	0.659089	110.1	0.710145	118.6	0.494317	82.6
4	0.63124	0.703183	111.4	0.744956	118	0.547693	86.8
6	0.691579	0.737994	106.7	0.777446	112.4	0.589467	85.2
8	0.728711	0.761201	104.5	0.78905	108.3	0.605712	83.1
10	0.737994	0.770484	104.4	0.807616	109.4	0.610353	82.7

ageing.

Hardness and 100% modulus (Tables 5 and 6) of silicone rubber nanocomposites demonstrated modest increase at the start of the ageing process, followed by a general declining tendency, similar to the tensile strength behaviour *vs*. ageing temperature. The unaged sample's hardness increased from 60 shore A to 61 shore A in the aged sample at 70 ℃, to 63 Shore A in the aged sample at 100 ℃, and then decreased to 58 Shore A. Similarly, the 100% modulus increased from 2.45 MPa in the unaged sample to 2.76 MPa in the 70 ℃ aged sample, 2.94 MPa in the 100 ℃ aged sample, and then dropped to 1.96 MPa in the 125 ℃ aged sample. Tables 5 and 6 show that during the early phases of exposure to high temperature, silicone rubber gets harder, resulting in increased 100% modulus and hardness, before becoming flexible compound and losing its capacity to resist indentation or penetration as the ageing progresses. In a investigation on thermal oxidation ageing of SR by Wu *et al.*,[61] they found an increasing trend in the rubber's 100% modulus, hardness, and compression set as a function of temperature (ageing temperature range of 120-180 ℃) and time (ageing time range of 45-81 h). The observed increasing-decreasing T_a and H_d pattern points to a conflict between ongoing crosslinking in the rubber and macromolecule chain disintegration.[61] Crosslinking may be encouraged early in the exposure, but breakdown of the polymer chains after 100 ℃ may overcome it.

T_a of elastomeric materials is crucial in a variety of developments and end-use items. In some cases, the life-limiting failure mechanism is tear fatigue. The T_a can be utilised to determine the elastomeric material's susceptibility to pre-existing flaws.[62] Tearing in these materials is mainly caused by faults in the compound itself, such as additives, imperfections in the mould surfaces, filler agglomerates and natural impurities in the obtained rubber. The local stress in the location of the flaw is exacerbated when the elastomer is stretched. When the stress reaches a critical point, the fracture (defect) extends farther, causing the rubber to rupture.[63] The SR nanocomposites employed in the current study are continually prone to tearing due to direct contact with metallic parts, which occasionally have rather sharp edges. As a result, it's critical to keep track of the T_a of SR nanocomposites exposed to high-temperature MDI-GO during this process. The T_a of SR nanocomposite varies with ageing temperature, as shown in Table 7. The T_a of SR nanocomposites improved marginally after 70 ℃ ageing, increasing by around 2%. However, as the rubber ages beyond 70 ℃, its tear strength begins to deteriorate, and it eventually loses 11% of its initial tear strength. As a result of extended exposure to the MDI-GO at high temperatures, the tear strength of silicone rubber nanocomposites deteriorates dramatically.

The changes in rebound resilience *vs*. ageing temperatures for silicone rubber nanocomposites with varying MDI-GO loading are shown in Table 8. The data are typically consistent, indicating that the rebound resilience test is sensitive and repeatable enough to identify thermal damage. It is obvious that when ageing temperatures rise, the rebound resilience value of each type of filled compound falls. This is related to the production of strong crosslinks and the oxidising skin that comes from oxygen uptake at the specimen's surface.[64] As a result, as the ageing temperature rises, the rebound resilience of nanocomposites decreases.

The crosslink density of the silicone rubber nanocomposites was considered from the M_{100} by means of the kinetic theory of elasticity.[65] $\sigma/(\lambda-(1/\lambda^2)$RT was used to calculate crosslink density (υ).[66-67] Where, λ, σ, R, and T are the extension ratio, M_{100}, gas constant and absolute temperature, respectively. Abrasion loss of thermally aged peroxide cured silicone rubber nanocomposites is plotted in Table 10 as a function of MDI-GO content. All of the nanocomposites show an increase in abrasion resistance after being thermally aged at 70 ℃. As demonstrated by the υ values in Table 9, this is attributable to the formation of additional crosslinks during thermal ageing process. The development of additional crosslinks is promoted when silicone rubber nanocomposites are thermally aged at 100 ℃. After ageing at 125 ℃, however, all samples' abrasion resistance declines. This is due to crosslink deterioration at high temperatures, as demonstrated by the υ values in Table 9.

Morphology. The morphology of the PSR nanocomposites shown in Figure 13, where Figure 13(a) shows silicone rubber nanocomposites with 6 phr MDI-GO and Figure 13(b) shows silicone rubber nanocomposites with the addition of 10 phr MDI-GO, could explain the reduction in elongation at break and tensile strength. Figure 13(a) clearly reveals that 6 phr MDI-GO has superior filler dispersion than 10 phr MDI-GO in Figure 13(b), owing to better rubber-filler interactions. The silicone rubber nanocomposites' tensile characteristics improved consequently of the greater dispersion and higher surface area of MDI-GO nanofillers. Figure 13(b) shows that the 10 phr MDI-GO nanofillers and the silicone rubber matrix have poor interfacial compatibility, resulting in visible voids inside the nanocomposites.

The morphology of the unaged and thermally aged PSR

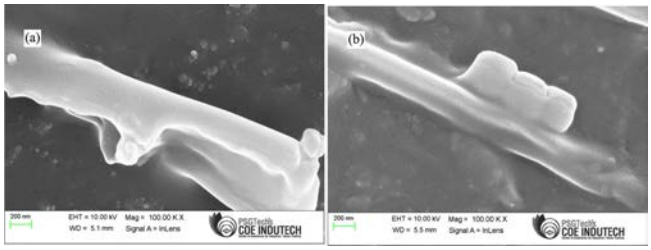

Figure 13. Tensile fractured surfaces of MDI-GO filled silicone rubber composites: (a) GO_6; (b) GO_{10}.

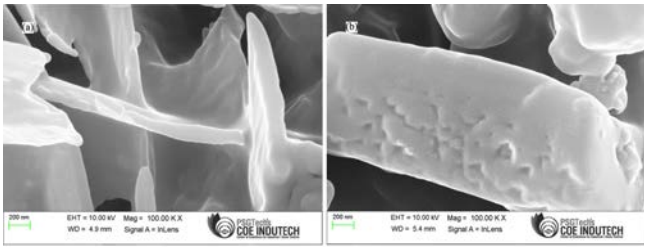

Figure 14. FESEM micrographs of (a) MDI-GO_6 fracture surface; (b) MDI-GO_{10} fracture surface of thermally aged PSR sample.

samples was investigated using FESEM. Figures 13 and 14, which are FESEM micrographs of fractured surfaces of thermally unaged and aged samples, respectively, indicate no appreciable differences in the surface morphology of the thermally aged samples (Figure 14) in comparison to the unaged samples (Figure 13). Different fracture mechanisms for the thermally unaged and aged samples are shown in FESEM pictures of the fractured surfaces of the samples, which were obtained via tensile tests. Large elastic regions protruded from the fracture surface of the unaged sample, demonstrating the material's strong elasticity at the time of fracture. The older sample, however, had a considerably flatter and more fragile surface. Figure 14 (a), (b) shows a few small cracks that seem to start from the PSR's surface texture. This increases the worry that as the surface ages, it may have stress-concentrated areas where cracks start more quickly.

Conclusions

The review of the MDI-GO and its suitability for use as filler in silicone rubber nanocomposites was the aim of this work. In this investigation, the use of MDI-GO as a filler in silicone rubber nanocomposites is advised to prevent the harmful impacts of the substance on the environment. It has been demonstrated that the addition of MDI-GO significantly improves the physical properties of silicone rubber.

The following conclusions can be taken from this study:

(1) The incorporation of MDI-GO into silicone rubber gradually increases tensile strength and elongation at break until a maximum is attained at 6 phr. Any additional filler rises causes the elongation at break and tensile strength to gradually diminish.

(2) Hardness increases with increasing MDI-GO content in rubber compound. The abrasion loss increases with increasing MDI-GO content. The dependency of hardness on filler content is very similar to that of abrasion resistance.

(3) There is a gradual decrease in resilience with increasing MDI-GO loading. The incorporation of MDI-GO nanofiller into the silicone rubber nanocomposites reduces the rebound resilience.

(4) 100% modulus of silicone rubber nanocomposites increases with increasing MDI-GO loading. Compression set increases with increasing MDI-GO loading.

(5) Minimum torque and maximum torque is steadily increased at 8 phr and is decreased above 8 phr of MDI-GO content, while CRI increased with increasing MDI-GO loading. Scorch and optimum cure time is initially decreased at lower content 8 phr and 6 phr and is increased above 8 phr and 6 phr of MDI-GO content, respectively.

(6) As filler loading is increased, the swelling ratio decreases. As a result of silicone nanocomposites loaded with MDI-GO having a higher cross-link density, the mole percent uptake was lower.

(7) The loading of MDI-GO particles also influences the accelerated ageing behaviour of silicone rubber nanocomposites at 70, 100, and 125 ℃ for 96 h.

According to the findings taken as a whole, 6 phr MDI-GO has the potential to be used as a black filler in silicone rubber composites. On the other hand, to achieve better reinforcement, lower content of MDI-GO particles should be used.

Conflict of Interest: The authors declare that there is no conflict of interest.

References

1. Fink, H.; Panne, U.; Niessner, R. Process Analysis of Recycled Thermoplasts from Consumer Electronics by Laser-induced Plasma Spectroscopy. *Anal. Chem.* **2002**, 74, 4334-4342.
2. Halley, P. J.; Mackay, M. E. Chemorheology of Thermosets—an Overview. *Polym. Eng. Sci.* **1996**, 36, 593-609.
3. Sundar, R.; Mohan, S. K.; Vishvanathperumal, S. Effect of Surface Modified Halloysite Nanotubes (mHNTs) on the Mechanical Properties and Swelling Resistance of EPDM/NBR Nanocomposites. *Polym. Korea* **2022**, 46, 728-743.
4. Vishvanathperumal, S.; Anand, G. Effect of Nanosilica on the Mechanical Properties, Compression Set, Morphology, Abrasion and Swelling Resistance of Sulphur Cured EPDM/SBR Composites.

Silicon **2022**, 14, 3523-3534.
5. Warrick, E. L.; Pierce, O. R.; Polmanteer, K. E.; Saam, J.C. Silicone Elastomer Developments 1967-1977. *Rubber Chem. Technol.* **1979**, 52, 437-525.
6. Gottenbos, B.; van der Mei, H.C.; Klatter, F.; Nieuwenhuis, P.; Busscher, H.J. *In Vitro* and *In Vivo* Antimicrobial Activity of Covalently Coupled Quaternary Ammonium Silane Coatings on Silicone Rubber, *Biomaterials* **2002**, 23, 1417-1423.
7. Harris, A. K.; Wild, P.; Stopak, D. Silicone Rubber Substrata: a New Wrinkle in the Study of Cell Locomotion, *Science* **1980**, 208, 177-179.
8. Chen, W. J.; Zeng, X.; Lai, X.; Li, H.; Fang, W. Z.; Hou, F. Suppression Effect and Mechanism of Platinum and Nitrogen-containing Silane on the Tracking and Erosion of Silicone Rubber for High-voltage Insulation, *ACS Appl. Mater. Interfaces* **2016**, 8, 21039-21045.
9. Berahman, R.; Raiati, M.; Mazidi, M. M.; Paran, S. M. R. Preparation and Characterization of Vulcanized Silicone Rubber/halloysite Nanotube Nanocomposites: Effect of Matrix Hardness and HNT Content, *Mater. Des.* **2016**, 104, 333-345.
10. Anand, G.; Vishvanathperumal, S. Properties of SBR/NR Blend: The Effects of Carbon Black/Silica (CB/SiO_2) Hybrid Filler and Silane Coupling Agent. *Silicon* **2022**, 14, 9051-9060.
11. Senthilvel, K.; Vishvanathperumal, S.; Prabu, B.; John Baruch, L. Studies on the Morphology, Cure Characteristics and Mechanical Properties of Acrylonitrile Butadiene Rubber with Hybrid Filler (carbon black/silica) Composite. *Polym. Polym. Compos.*, **2016**, 24, 473-480.
12. Wu, W.; Chen, D. Thermal and Mechanical Properties of Silicon Rubber/cispolybutadiene Rubber/ethylene-propylene-diene Monomer Blends, *J. Appl. Polym. Sci.* **2006**, 101, 4462-4467.
13. Iijima, S. Helical Microtubules of Graphitic Carbon. *Nature* **1991**, 354, 56-58.
14. Geim, A. K. Graphene: Status and Prospects. *Science* **2009**, 324, 1530-1534.
15. Galimberti, M., Cipolletti, V., Musto, S., Cioppa, S., Peli, G., Mauro, M., Gaetano, G., Agnelli, S., Theonis, R. and Kumar, V. Recent Advancements in Rubber Nanocomposites. *Rubber Chem. Technol.* **2014**, 87, 417-442.
16. Novoselov, K. S.; Fal′ko, V. I.; Colombo, L.; Gellert, P. R.; Schwab, M. G.; Kim, K. A Roadmap for Graphene, *Nature* **2012**, 490, 192.
17. Allen, M. J.; Tung, V. C.; Kaner, R. B. Honeycomb Carbon: a Review of Graphene. *Chem. Rev.* **2010**, 110, 132-45.
18. Gao, W.; Alemany, L. B.; Ci, L.; Ajayan, P. M. New Insights Into the Structure and Reduction of Graphite Oxide. *Nat. Chem.* **2009**, 1, 403-408.
19. Ren, P. G.; Yan, D. X.; Ji, X.; Chen, T.; Li, Z. M. Temperature Dependence of Graphene Oxide Reduced by Hydrazine Hydrate. *Nanotechnology* **2010**, 22, 055705.
20. Liu, X.; Kuang, W.; Guo, B. Preparation of Rubber/graphene Oxide Composites with In-situ Interfacial Design. *Polymer* **2015**, 56, 553-562.
21. Tang, X.; Li, W.; Yu, Z. Enhanced Thermal Stability in Graphene Oxide Covalently Functionalized with 2-amino-4,6-didodecylamino-1,3,5-triazine. *Carbon*. **2011**, 49, 1258-1265.
22. Yu, W.; Xie, H. Highly Efficient Method for Preparing Homogeneous and Stable Colloids Containing Graphene Oxide. *Nanoscale Res. Lett.* **2011**, 6, 47.
23. Tessonnier, J.; Barteau, M. Dispersion of Alkyl-Chain-Functionalized Reduced Graphene Oxide Sheets in Nonpolar Solvents. *Langmuir*. **2012**, 28, 6691-6697.
24. Huang, Y.; Yan, W.; Huang, L.; Chen, Y. Functionalization of Graphene Oxide by Two-Step Alkylation. *Macromol. Chem. Phys.* **2012**, 213, 1101-1106.
25. Kim, H.; Miura, Y.; Macosko, C. W. Graphene/Polyurethane Nanocomposites for Improved Gas Barrier and Electrical Conductivity, *Chem. Mater.* **2010**, 22, 3441-3450.
26. Deshmukh, K.; Joshi, G. M. Thermo-mechanical Properties of Poly(vinyl chloride)/graphene Oxide as High Performance Nanocomposites, *Polym. Test.* **2014**, 34, 211-219.
27. Wang, X.; Dou, W. Preparation of Graphite Oxide (GO) and the Thermal Stability of Silicone Rubber/GO Nanocomposites, *Thermochimica Acta* **2012**, 529, 25-28.
28. Ozbas, B.; O'Neill, C. D.; Register, R. A.; Aksay, I. A.; Prud'homme, R. K.; Adamson, D. H. Multifunctional Elastomer Nanocomposites with Functionalized Graphene Single Sheets. *J. Polym. Sci. Part B: Polym. Phys.* **2012**, 50, 910-916.
29. Gan, L.; Shang, S. M.; Yuen, C. W. M.; Jiang, S. X.; Luo, N. M. Facile Preparation of Graphene Nanoribbon Filled Silicone Rubber Nanocomposite with Improved Thermal and Mechanical Properties, *Compos. Part B: Eng.* **2015**, 69, 237-242.
30. Shan, C.; Yang, H.; Song, J.; Han, D.; Ivaska, A.; Niu, L. Direct Electrochemistry of Glucose Oxidase and Biosensing for Glucose Based on Graphene, *Anal. Chem.* **2009**, 81, 2378-2382.
31. Mukhopadhyay, S.; Dutta, S. Comparison of Solid State and Sol-gel Derived Calcium Aluminate Coated Graphite and Characterization of Prepared Refractory Composite, *Ceramics International* **2012**, 38, 4997-5006.
32. Castarlenas, S.; Rubio, C.; Mayoral, Á.; Téllez, C.; Coronas, J. Few-layer Graphene by Assisted-exfoliation of Graphite with Layered Silicate, *Carbon* **2014**, 73, 99-105.
33. Yoon, K. Y.; An, S. J.; Chen, Y.; Lee, J. H.; Bryant, S. L.; Ruoff, R. S.; Huh, C.; Johnston, K. P. Graphene Oxide Nanoplatelet Dispersions in Concentrated NaCl and Stabilization of Oil/water Emulsions, *J. Colloid Interface Sci.* **2013**, 403, 1-6.
34. Liu, Z.; Wang, Y.; Zhang, X.; Xu, Y.; Chen, Y.; Tian, J. Nonlinear Optical Properties of Graphene Oxide in Nanosecond and Picosecond Regimes. *Appl. Phys. Lett.* **2009**, 94, 021902.
35. Bai, J.; Liao, X.; Huang, E.; Luo, Y.; Yang, Q.; Li, G. Control of the Cell Structure of Microcellular Silicone Rubber/nanographite Foam for Enhanced Mechanical Performance, *Mater. Des.* **2016**, 133, 288-298.
36. Gan, L.; Shang, S.; Jiang, S. X. Impact of Vinyl Concentration of a Silicone Rubber on the Properties of the Graphene Oxide Filled Silicone Rubber Composites. *Compos. Part B: Eng.* **2016**, 84,

294-300.
37. An, K.; Peng, S.; Yang, C.; Qing, Y.; Hu, C.; Wabg, L.; Liu, C. Covalent Modification of Graphene Oxide by 4,4′-methylenebis (phenyl isocyanate) to Enhance Corrosion Resistance of Polystyrene Coating. *Colloid Polym. Sci.* **2019**, 297, 839-848.
38. Vishvanathperumal, S.; Gopalakannan, S. Swelling Properties, Compression Set Behavior and Abrasion Resistance of Ethylene-propylene-diene Rubber/styrene Butadiene Rubber Blend Nanocomposites. *Polym. Korea* **2017**, 41, 433-442.
39. Vishvanathperumal, S.; Navaneethakrishnan, V.; Gopalakannan, S. The Effect of Nanoclay and Hybrid Filler on Curing Characteristics, Mechanical Properties and Swelling Resistance of Ethylene-vinyl Acetate/styrene Butadiene Rubber Blend Composite. *J. Adv. Microscopy Res.* **2018**, 13, 469-476.
40. Vishvanathperumal, S.; Gopalakannan, S. Effects of the Nanoclay and Crosslinking Systems on the Mechanical Properties of Ethylene-propylene-diene Monomer/styrene Butadiene Rubber Blends Nanocomposite. *Silicon* **2019**, 11, 117-135.
41. Song, S. H.; Jeong, H. K.; Kang, Y. G. Preparation and Characterization of Exfoliated Graphite and Its Styrene Butadiene Rubber Nanocomposites. *J. Ind. Eng. Chem.* **2010**, 16, 1059-1065.
42. Yang, J.; Tian, M.; Jia, Q. X.; Zhang, L. Q.; Li, X. L. Influence of Graphite Particle Size and Shape on the Properties of NBR. *J. Appl. Polym. Sci.* **2006**, 102, 4007-4015.
43. Yang, J.; Tian, M.; Jia, Q. X.; Shi, J. H.; Zhang, L. Q.; Lim, S. H.; Yu, Z. Z.; Mai, Y. W. Improved Mechanical and Functional Properties of Elastomer/graphite Nanocomposites Prepared by Latex Compounding. *Acta Materialia* **2007**, 55, 6372-6382.
44. Vishvanathperumal, S.; Anand, G. Effect of Nanoclay/nanosilica on the Mechanical Properties, Abrasion and Swelling Resistance of EPDM/SBR Composites. *Silicon* **2020**, 12, 1925-1941.
45. Ganeche, P. S.; Balasubramanian, P.; Vishvanathperumal, S.; Halloysite Nanotubes (HNTs)-filled Ethylene-propylene-diene Monomer/styrene-butadiene Rubber (EPDM/SBR) Composites: Mechanical, Swelling, and Morphological Properties. *Silicon* **2022**, 14, 6611-6620.
46. Smith, L. P. *The Language of Rubber: An Introduction to the Specification and Testing of Elastomers*; Butterworth-Heinemann: Oxford, 1993.
47. Othman, A. B.; Property Profile of a Laminated Rubber Bearing. *Polym. Test.* **2001**, 20, 159-166.
48. Vishvanathperumal, S.; Anand, G. Effect of Nanosilica and Crosslinking System on the Mechanical Properties and Swelling Resistance of EPDM/SBR Nanocomposites with and Without TESPT. *Silicon* **2021**, 13, 3473-3497.
49. Davies, B. Longest Serving Polymer. *Rubber Developments* **1988**, 41, 102-9.
50. Ravi Theja, M. S.; Kilari, N.; Vishvanathperumal, S.; Navaneethakrishnan, V. Modeling Tensile Modulus of Nanoclay-filled Ethylene-propylene-diene Monomer/styrene-butadiene Rubber Using Composite Theories. *J. Rubber Res.* **2021**, 24, 847-856.
51. Ngolemasango, F. E.; Bennett, M.; Clarke, J. Degradation and Life Prediction of a Natural Rubber Engine Mount Compound. *J. Appl. Polym. Sci.* **2008**, 110, 348-355.
52. Chou, H.-W.; Huang, J.-S. Effects of Ultraviolet Irradiation on the Static and Dynamic Properties of Neoprene Rubbers. *J. Appl. Polym. Sci.* **2008**, 110, 2907-2913.
53. Chou, H.-W.; Huang, J.-S. Effects of Cyclic Compression and Thermal Aging on Dynamic Properties of Neoprene Rubber Bearings. *J. Appl. Polym. Sci.* **2008**, 107, 1635-1641.
54. Chou, H.-W.; Huang, J.-S.; Lin, S.-T. Effects of Thermal Aging on Fatigue of Carbon Black-Reinforced EPDM Rubber. *J. Appl. Polym. Sci.* **2007**, 103, 1244-1251.
55. Clough, R. L.; Gillen, K. T. Degradation Mechanisms and Accelerated Aging Test Design; Sandia National Labs: Albuquerque, 1985.
56. Wu, J.; Dong, J.; Wang, Y.; Gond, B. K. Thermal Oxidation Ageing Effects on Silicone Rubber Sealing Performance. *Polym. Degrad. Stab.* **2017**, 135, 43-53.
57. Brüning, K. In-Situ Structure Characterization of Elastomers During Deformation and Fracture; Springer: Cham, 2014.
58. Brown, R. P. *Physical Testing of Rubbers*. 3rd ed. Chapman and Hall London, 1996; p. 74.
59. Clarke, J.; Ngolemasango, E. F.; Bennett, M. Kinetics of the Effect of Ageing on Tensile Properties of a Natural Rubber Compound. *J. Appl. Polym. Sci.* **2006**, 102, 3732-3740.
60. Vishvanathperumal, S.; Navaneethakrishnan, V.; Anand, G.; Gopalakannan, S. Evaluation of Crosslink Density Using Material Constants of Ethylene-propylene-diene Monomer/styrene-butadiene Rubber with Different Nanoclay Loading: Finite Element Analysis-simulation and Experimental. *Adv. Sci., Eng. Med.* **2020**, 12, 632-642.
61. Wu, J.; Dong, J.; Wang, Y.; Gond, B.K. Thermal Oxidation Ageing Effects on Silicone Rubber Sealing Performance. *Polym. Degrad. Stab.* **2017**, 135, 43-53.
62. Bernardi, L.; Hopf, R.; Sibilio, D.; Ferrari, A.; Ehret, A. E.; Mazza, E. On the Cyclic Deformation Behavior, Fracture Properties and Cytotoxicity of Silicone-Based Elastomers for Biomedical Applications. *Polym. Test.* **2017**, 60, 117-123.
63. Sakulkaew, K.; Thomas, A. G.; Busfield, J. J. C. The Effect of the Rate of Strain on Tearing in Rubber. *Polym. Test.* **2011**, 30, 163-172.
64. Brown, R. P.; Soulagnet, G. Microhardness Profiles on Aged Rubber Compounds. *Polym. Test.* **2001**, 20, 295-303.
65. Blow, C. M.; Hepburn, C. *Rubber Technology and Manufacture*, 2nd ed.; Butterworths: London, 1981.
66. Radhakrishnan, C. K.; Alex, R.; Unnikrishnan, G. Thermal, Ozone and Gamma Ageing of Styrene Butadiene Rubber and Poly (ethylene-*co*-vinyl acetate) Blends. *Polym. Degrad. Stab.* **2006**, 91, 902-910.
67. Vishvanathperumal, S.; Gopalakannan, S. Reinforcement of Ethylene Vinyl Acetate with Carbon Black/silica Hybrid Filler Composites. *In Appl. Mechanics Mater.* **2016**, 852, 16-22.